

The Conformational Origin of the Barrier to the Formation of Neighboring Group Assistance in Glycosylation Reactions: A Dynamical Density Functional Theory Study

Attila Bérces,^{1a} Gary Enright,^{1a} Tomoo Nukada,^{1b} and Dennis M. Whitfield^{*,1c}

Contribution from the Steacie Institute for Molecular Sciences, National Research Council Canada, 100 Sussex Dr., Ottawa, Ontario K1A 0R6, Canada, The Institute for Physical and Chemical Research (RIKEN), Wako-shi, Saitama 351-01, Japan, and Institute for Biological Sciences, National Research Council Canada, 100 Sussex Dr., Ottawa, Ontario K1A 0R6, Canada

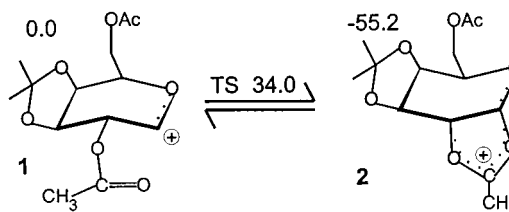
Received April 5, 2000. Revised Manuscript Received April 2, 2001

Abstract: Static and dynamical Density Functional Theory studies of 2,6-di-*O*-acetyl-3,4-*O*-isopropylidene- β -D-galactopyranosyl cation have shown that this cation can exist in two conformers characterized as ²S_O and B_{2,5}, respectively. The ²S_O conformer has the O-2 acyl group equatorial with the carbonyl syn to H-2 and is populated by monocyclic oxocarbenium ions. These conformational features are present in the structurally related glycosyl donor ethyl 2,6-di-*O*-benzoyl-3,4-*O*-isopropylidene- β -D-galactothiopyranoside as determined by X-ray diffraction studies. The B_{2,5} conformer has O-2 axial and allows the carbonyl to rotate and close the five-membered ring to form a bicyclic dioxolenium ion. Constraints based on natural internal coordinates were implemented to study this conformational transition. In this way the barrier to interconversion has been determined to be 34 kJ mol⁻¹ with a transition state characterized as ⁰S₂ and a pathway involving pseudorotation. Thus, for the first time the structures and energetics of the key ions postulated to be involved in neighboring group assisted glycosylation reactions have been determined.

Introduction

Winstein and co-workers first interpreted the stereochemical outcome of substitution reactions of 1,2-disubstituted cyclohexanes in terms of neighboring group assistance.² Carbohydrate chemists realized that these concepts rationalized some of the complexities of glycosylation reactions with *O*-acyl groups adjacent to the reactive anomeric center.³ In particular, stereochemical control of some glycosylation reactions and anchimeric assistance of poor leaving groups are accounted for.⁴ The monocyclic **1** and the bicyclic **2** oxocarbenium ions are essential precursors of the neighboring group assisted glycosylation, see Scheme 1. The predominant formation of *trans*-glycosides is usually rationalized by an S_N2-like reaction at the anomeric carbon of ions such as **2**.^{5,6} However, such a mechanism is inconsistent with the postulate of Dewar that pentacoordinate S_N2 transition states adjacent to an oxygen atom are antiaromatic.⁷ In addition, the positive charge is on the former carbonyl carbon of **2** which makes the anomeric carbon an unlikely reaction center.⁸

Scheme 1. Intermediates **1** and **2** in the Neighboring Group Assisted Glycosylation Reaction of the 2,6-Di-*O*-acetyl Analogue of **3** (Energies in kJ Mol⁻¹)



Our recent study of a particular neighboring group assisted glycosylation reaction offers an alternative interpretation of the stereochemistry based on the relative energies of the α and β intermediates formed by a direct S_N1-like attack on the oxocarbenium ion **1**.⁹ However, **1** is thermodynamically unstable with respect to cyclization (cf. **2**) and thus we needed to study its kinetic stability to evaluate this hypothesis. In this report we explore the reaction pathway that connects **1** to **2** by constrained ab initio molecular dynamics methods. Crucial questions are whether the reaction is stepwise or concerted and ultimately if there is a significant energy barrier.

Computational Details

Constrained geometry dynamics require the definition of constraints that have a high projection on the reaction coordinate. Molecular mechanics simulations often use internal coordinates, like bond length, bond angles, and dihedral angles, as constraints.¹⁰ We derived constraints based on the natural internal

(1) (a) Steacie Institute for Molecular Sciences (NRC); present address of A. Bérces: Novartis Forschungsinstitut GmbH, Brunner Strasse 59, A-1235 Vienna, Austria. (b) RIKEN. (c) Institute for Biological Sciences (NRC).

(2) Winstein, S.; Buckles, R. E. *J. Am. Chem. Soc.* **1942**, *64*, 2780.

(3) (a) Frush, H. L.; Isbell, H. S. *J. Res. Natl. Bur. Stand.* **1941**, *27*, 413.

(b) Pascu, E. *Adv. Carbohydr. Chem.* **1945**, *1*, 77.

(4) Lemieux, R. U. *Adv. Carbohydr. Chem.* **1954**, *9*, 1.

(5) Whitfield, D. M.; Douglas, S. P. *Glycoconj. J.* **1996**, *13*, 5.

(6) (a) Banoub, J.; Bundle D. R. *Can. J. Chem.* **1979**, *57*, 2091. (b) Magnus, V.; Vikić-Topić, D.; Iskrčić, S.; Kveder, S. *Carbohydr. Res.* **1983**, *114*, 209.

(7) Dewar, M. J. S.; Dougherty R. C. *The PMO Theory of Organic Chemistry*; Plenum Publishing Corp.: New York, 1975; p 263.

(8) Nukada, T.; Bérces, A.; Zgierski, M. Z.; Whitfield, D. M. *J. Am. Chem. Soc.* **1998**, *120*, 13291.

(9) Nukada, T.; Bérces, A.; Whitfield, D. M. *J. Org. Chem.* **1999**, *64*, 9030.

coordinate representation of the conformational degrees of freedom.¹¹ A distortion from the planar structure into the ¹C₄ chair conformation is represented by

$$q_1 = \tau_1 - \tau_2 + \tau_3 - \tau_4 + \tau_5 - \tau_6 \quad (1)$$

internal coordinate where τ_1 , τ_2 , τ_3 , τ_4 , τ_5 , and τ_6 stand for the dihedral angles defined by the C-1C-2C-3C-4, C-2C-3C-4C-5, C-3C-4C-5-O, C-4C-5-OC-1, C-5OC-1C-2, and OC-1C-2C-3 atom sets, respectively. Similarly, internal coordinates corresponding to the ^{1,4}B boat (q_2) and ^OS₂ twist-boat (q_3) conformations can be defined as

$$q_2 = \tau_2 - \tau_3 - \tau_5 + \tau_6 \quad (2)$$

and

$$q_3 = \tau_1 - \frac{1}{2}\tau_2 - \frac{1}{2}\tau_3 + \tau_4 - \frac{1}{2}\tau_5 - \frac{1}{2}\tau_6 \quad (3)$$

respectively.

The internal coordinates defined in eqs 1 through 3 can define any conformation of a six-membered ring. The chair distortion coordinate can also be used to represent one of the common conformational pathways, the chair inversion pathway. The other common pathway is the pseudorotational pathway that involves both boat- and twist-boat-type distortions. The pseudorotation is a consequence of the degenerate nature of the boat and twist-boat distortions in the highest symmetry limit. The pseudorotation is best represented by the phase angle defined by the boat and twist-boat coordinates, q_2 and q_3 :

$$\phi = \alpha \tan(\sqrt{3}q_2/2q_3) \quad (4)$$

The $\sqrt{3}/2$ term arises from normalization factors. Equation 4 is consistent with the Cremer Pople definition of ϕ , provided the ring atoms are numbered by carbohydrate numbering. The zero value of the phase angle corresponds to the ^{1,4}B conformation. All conformations of six-membered rings use the IUPAC recommended nomenclature and were determined as described in a recent report.¹²

We implemented the conformational constraints in constrained ab initio molecular dynamics in the Projector Augmented Wave method (PAW, See details below). The implementation of the constraints in ab initio molecular dynamics follows the SHAKE algorithm.¹⁰ This algorithm had been implemented in the PAW program package for several other constraints. Our implementation required new subroutines that calculate the value and the derivatives with respect to Cartesian atomic coordinates of the coordinates defined in eqs 1 through 4.

Static DFT Calculations. The reported static calculations were carried out with the Amsterdam Density Functional (ADF) program system version 2.3 derived from the work of Baerends et al.¹³ and developed at the Free University of Amsterdam^{14,15}

(10) Ryckaert, J.-P.; Ciccotti, G.; Berendsen, H. J. C. *J. Comput. Phys.* **1997**, *23*, 327.

(11) Forgasi, G.; Zhou, X.; Taylor, P. W.; Pulay, P. *J. Am. Chem. Soc.* **1992**, *114*, 8191.

(12) Bérces, A.; Whitfield, D. M.; Nukada, T. *Tetrahedron* **2001**, *57*, 477.

(13) Baerends, E. J.; Ellis, D. E.; Ros, P. *Chem. Phys.* **1973**, *2*, 41.

(14) Ravenek, W. In *Algorithms and Applications on Vector and Parallel Computers*; te Riele, H. J. J., Dekker, Th. J., van de Vorst, H. A., Eds.; Elsevier: Amsterdam, The Netherlands, 1987.

(15) (a) Boerrigter, P. M.; te Velde, G.; Baerends, E. J. *Int. J. Quantum Chem.* **1988**, *33*, 87. (b) te Velde, G.; Baerends, E. J. *J. Comput. Phys.* **1992**, *99*, 84.

and the University of Calgary.¹⁶ The energy functional in all static calculations used the local density approximation¹⁷ (LDA) augmented with gradient corrections to the exchange and correlation potentials by Becke¹⁸ and Perdew.¹⁹

The atomic orbitals were described by an uncontracted double- ζ Slater function basis set²⁰ augmented by a single- ζ polarization function. The 1s² configuration on carbon and oxygen was assigned to the core and treated by the frozen-core approximation. The electron density was fitted to a set of s, p, d, f, and g Slater functions centered on all nuclei to calculate the Coulomb and exchange potentials accurately in each SCF cycle.²¹ A continuum dielectric constant method described previously was used to estimate solvation effects.⁸ The probe radius 2.4 Å and the dielectric constant of $\epsilon = 9.0$ corresponds to CH₂Cl₂ which was a typical solvent for the glycosylation reactions. These calculations were carried out on a multiprocessor SGI Origin 2000 workstation.

Dynamical DFT Calculations. Dynamical DFT calculations were carried out with the PAW method,²² an implementation of the Car–Parrinello ab initio molecular dynamics²³ by Blöchl. This method uses an augmented plane wave basis set which allows one to describe the full all-electron wave function. The description of the core wave function takes advantage of the frozen core approximation. These simulations used an energy cutoff of 30 Rydberg for the plane wave basis set and periodic boundary conditions in a unit cell defined by lattice vectors ([0.0 10.0 10.0] [10.0 0.0 10.0] [10.0 10.0 0.0]) Å. Typically 132 grid points were used in each dimension of the periodic cell. All calculations employed the exchange correlation functional of the generalized gradient approximation with the local potential of Perdew and Zunger²⁴ augmented by the gradient corrections to the exchange and correlation of Becke¹⁷ and Perdew.¹⁸ To prevent electrostatic interactions between periodic images, a charge isolation scheme was used.²⁵ The nuclei were brought to a temperature of 300 K by applying a sequence of 50–150 sinusoidal pulses of excitation vectors orthogonal to the already excited modes. A temperature of 300 K was maintained for all simulations by a Nosé thermostat^{26,27} to simulate a canonical (NVT) ensemble. The fictitious kinetic energy of the electrons was controlled in a similar fashion by a Nosé thermostat.²⁸ We used mass re-scaling to 2.0 (O and C) and 1.5 (H) atomic mass units to enable faster sampling combined with an integration time step of 7 au (0.17 fs). Since we do not discuss time-dependent properties and since configurational ensemble averages remain unchanged under a re-scaling of the masses, this technique is appropriate. To explore a reaction path we carried out constrained dynamics with the SHAKE algorithm.¹⁰ It is desirable that the constraint has a high projection onto the intrinsic reaction coordinate (IRC).²⁹ All other degrees of

(16) Fan, L.; Ziegler, T. *J. Phys. Chem.* **1992**, *96*, 6937.

(17) Vosko, S. H.; Wilk, L.; Nusair, M. *Can. J. Phys.* **1980**, *58*, 1200.

(18) Becke, A. D. *Phys. Rev. A* **1988**, *38*, 2398.

(19) Perdew, J. P. *Phys. Rev. B* **1986**, *33*, 8822; **1986**, *B34*, 7046.

(20) (a) Snijders, G. J.; Baerends, E. J.; Vernooijs, P. *At. Nucl. Data Tables* **1982**, *26*, 483. (b) Vernooijs, P.; Snijders, G. J.; Baerends, E. J. *Slater Type Basis Functions for the whole Periodic System*; Internal report, Free University of Amsterdam: Amsterdam, The Netherlands, 1981.

(21) Krijn, J.; Baerends, E. J. *Fit functions in the HFS-method*; Internal Report (in Dutch); Free University of Amsterdam: Amsterdam, The Netherlands, 1984.

(22) Blöchl, P. E. *Phys. Rev. B* **1994**, *50*, 17953.

(23) Car, R.; Parrinello, M. *Phys. Rev. Lett.* **1985**, *55*, 2471.

(24) Perdew, J. P.; Zunger, A. *Phys. Rev. B* **1981**, *23*, 5048.

(25) Blöchl, P. E. *J. Chem. Phys.* **1995**, *103*, 7422.

(26) Hoover, W. G. *Phys. Rev. A* **1985**, *31*, 1695.

(27) Nosé, S. *Mol. Phys.* **1984**, *52*, 255.

(28) Blöchl, P. E.; Parrinello, M. *Phys. Rev. B* **1992**, *45*, 9413.

(29) Fukui, K. *Acc. Chem. Res.* **1981**, *14*, 363.

freedom are allowed to evolve naturally in time. By slowly varying the constraint, the phase space in the vicinity of the TS can be sampled dynamically, leading to undisturbed dynamics for all motions that are orthogonal to the constraint. This “slow-growth” technique allows us to investigate reactions that would take place on a larger time scale than the simulations. Slow-growth simulations consist of 60 000 time steps and cover 10.2 ps real time, unless otherwise indicated in the text or figure captions. The free energy difference, ΔF , between two arbitrary points (λ_0 and λ_1) along the reaction coordinate λ can be evaluated by integrating the average force on λ at a given constant temperature T :

$$\Delta F = F(\lambda_1) - F(\lambda_0) = \int_{\lambda_0}^{\lambda_1} \langle \delta E / \delta \lambda \rangle_{\lambda, T} d\lambda \quad (5)$$

ΔF as derived by this formula does not rely on the harmonic approximation but it does not include quantum effects. For eq 5 to give the correct results, $\langle \delta E / \delta \lambda \rangle_{\lambda, T}$ must be determined at a large number of points between λ_0 and λ_1 . Furthermore, for each point, an extensive sampling is required at constant temperature T to determine the proper average $\langle \delta E / \delta \lambda \rangle_{\lambda, T}$. In the “slow growth” limit, λ is scanned continuously so that only a single value of $\langle \delta E / \delta \lambda \rangle_{\lambda, T}$ is determined at each value of λ . This method has the advantage of not disrupting the dynamics when the value of λ is changed. The slow growth method has been previously demonstrated on several elementary reaction steps in organometallic chemistry.³⁰ In the slow growth method the energy gradient is not averaged at constant values of λ , therefore it does not yield the free energy exactly. However, this method is successful for the qualitative understanding of the reaction mechanisms, the location of stationary points on the free energy surface, and semiquantitative calculation of free energy differences.

The two different implementations of DFT give similar relative energies. For example, the energy difference between **1** and **2** is -57.3 and -55.2 kJ mol⁻¹ by PAW and ADF, respectively.

Experimental Methods

Ethyl 2,6-di-*O*-benzoyl-3,4-*O*-isopropylidene- β -D-galactothiopyranoside, **3**, was prepared according to ref 9. A sample was recrystallized from ethanol/water to provide crystals suitable for X-ray diffraction studies. The full details are provided as tables of crystallographic data for **3** and are available free of charge via the Internet at <http://pubs.acs.org>.

Results and Discussion

The advantages of exploring reaction pathways by dynamical methods have been demonstrated in the literature.³¹ In the case of carbohydrates, this method is particularly appropriate for two reasons. Carbohydrates have a large number of conformations separated by relatively small barriers and it is almost hopeless to find all minima. However, a well executed dynamical calculation samples the conformational space at least to that extent that it prevents the structure from becoming locked into a high energy local minimum. Furthermore, the conformational transitions of sugar rings involve many elementary steps. Most reaction path following algorithms in quantum chemistry had

(30) Woo, T. K.; Margl, P. M.; Lohrenz, J. C. W.; Blöchl, P.; Ziegler, T. *J. Am. Chem. Soc.* **1996**, *118*, 13021.

(31) (a) Schwarz, K.; Nusterer, E.; Margl, P.; Blöchl, P. E. *Int. J. Quantum Chem.* **1997**, *61*, 369. (b) Blöchl, P. E.; Senn, H. M.; Togni, A. In *Transition State Modeling for Catalysis*; Truhlar, D. G., Morokuma, K., Eds.; American Chemical Society Symp. Ser. No. 721; American Chemical Society: Washington, DC, 1999; p 88.

Table 1. Calculated Barriers to Chair Inversion (in kJ mol⁻¹) at 300 K

compd	$\Delta H(\text{calcd})$	$\Delta H(\text{exptl})$	$\Delta G(\text{calcd})$	$\Delta G(\text{exptl})$
cyclohexane	48	50.6 \pm 2.0 ^a	41	43 ^b
tetrahydropyran	37	42.0 \pm 5.0 ^b	40	41.0 \pm 1.6 ^b
<i>m</i> -dioxane	44	40.0 \pm 2.1 ^b	38	41.0 \pm 0.8 ^b
<i>p</i> -dioxane	47	n.a.	47	\sim 41 ^b
<i>s</i> -trioxane	47	37.0 \pm 5.0 ^b	46	46.0 \pm 0.8 ^b

^a Reference 50. ^b Reference 51.

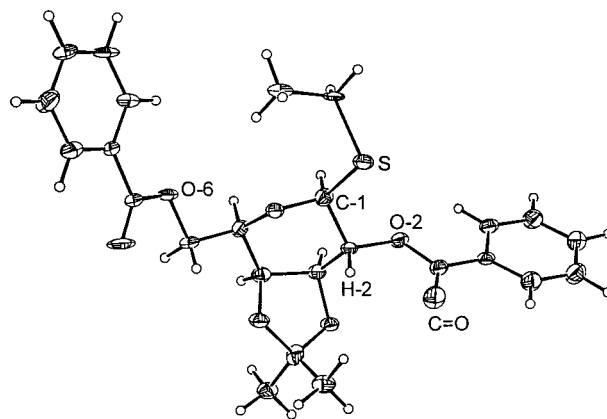


Figure 1. ORTEP representation of the X-ray structure of **3**.

been developed with elementary reaction steps in mind. To explore multistep reactions by considering elementary reaction steps creates an intractable combinatorial problem. Methods have been developed for the conformational analysis of small hydrocarbon rings³² including methods that particularly address pyranose conformations.³³ However, these methods are either too expensive³² or incompatible³³ with quantum chemical applications. For this reason we developed a new method to address this problem which is explained in the Computational Details section.

Benchmark tests on the enthalpy and the free energy barrier of chair inversion of some six-membered rings represent a remarkable agreement between experiment and theory for both quantities, see Table 1. For example, the lowering of the enthalpic barrier to inversion by oxygen substitution on going from cyclohexane to tetrahydropyran is well reproduced by calculation as well as the smaller difference in free energy. Complete details of these calculations will be given in a separate report.³⁴

With these tools we studied the interconversion of **1** and **2**. First we needed to know the conformational preferences of **1**. For this purpose we determined the X-ray crystal structure of the donor **3**, ethyl 2,6-di-*O*-benzoyl-3,4-*O*-isopropylidene- β -D-galactothiopyranoside. A representation of this structure is shown in Figure 1.³⁵ The pyranose ring conformation is a ⁴C₁ chair distorted toward a B_{1,4} boat conformation due to the fused 3,4-*O*-isopropylidene protecting group. The carbonyl of the 2-*O*-benzoyl is oriented syn to H-2, a usual conformation of esters.³⁶ Since the C-S bond is relatively long (1.802 Å), ionization is

(32) Kolossváry, I.; Guida, W. C. *J. Am. Chem. Soc.* **1993**, *115*, 2107.

(33) Ferro, D. R.; Provasoli, A.; Ragazzi, M. *Carbohydr. Res.* **1992**, *228*, 439.

(34) Bérces, A.; Nukada, T.; Whitfield, D. M. Unpublished observations.

(35) Crystallographic data (excluding structure factors) for the structure reported in this paper have been deposited with the Cambridge Crystallographic Data Centre as supplementary publication no. CCDC-138824. Copies of the data can be obtained free of charge on application to CCDC, 12 Union Road, Cambridge CB2 1EZ, UK (fax: (+44)1223-336-033; e-mail: deposit@ccdc.cam.ac.uk).

(36) Schweizer, W. B.; Dunitz, J. D. *Helv. Chim. Acta* **1982**, *65*, 1547.

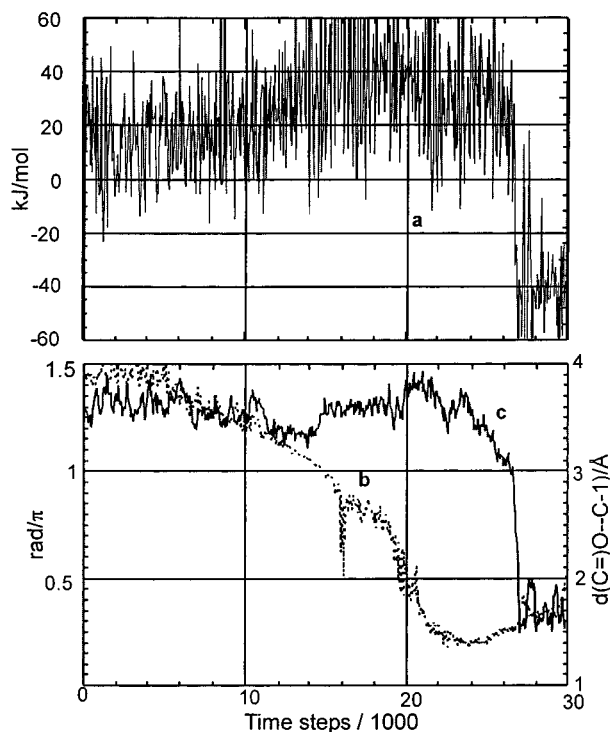


Figure 2. (a) Potential energy, (b) pseudorotation phase angle, and (c) (C=O)-C-1 distance during the dynamical trajectory.

anticipated to occur by lengthening of this bond followed by irreversible rearrangement of the alkylthio:promoter complex to yield an oxocarbenium ion like **1** in Scheme 1. Experimentally donor **3** yields predominantly β -glycosides as expected for donors capable of neighboring group participation.⁹ Previous static calculations found a 2S_0 conformation for **1** that maintains the syn and equatorial conformational features about the C-2-O-2 bond. The formation of the bicyclic intermediate, **2**, requires two significant conformational changes: the ring conformation has to change so that the 2-O-acyl protecting group moves from the equatorial position into an axial position and the acyl group has to rotate around the C-2-O-2 bond. Previous static calculations found a $B_{2,5}$ conformation for **2** that has O-2 axial and the dioxolenium ring closed. Although these reaction steps have been previously hypothesized, neither the energetic consequences nor the conformational preferences of such ions have been examined in detail. For example, Lemieux postulated a ${}^{1,4}B$ transition state for the process of ring inversion for the 2,3,4,6-tetra-*O*-acetyl-D-glucopyranosyl cation.³⁷ Also, the additional mechanistic question of whether ring inversion precedes acyl group rotation or not is raised.

The trajectory that we found to be the minimum energy path as determined by constrained ab initio molecular dynamics is described in Figure 2 in terms of potential energy (a), the pseudorotation phase angle in eq 4 (b), and the (C=O)-C-1 distance (c). Initially the trajectory follows the pseudorotational itinerary in a negative direction as indicated by the phase angle. It passes through the 2S_0 , ${}^{2,5}B$, 5S_1 , $B_{1,4}$, 3S_1 , ${}^{3,0}B$, 0S_2 , and $B_{2,5}$ conformations. Once the O-2 group is in an axial position, the dioxolene ring closure occurs spontaneously with little or no barrier as indicated by the sudden closure of the (C=O)-C-1 bond (see c in Figure 2 and Figure 3). Consequently, this is an asynchronous reaction where the conformational change dominates the reaction coordinate up to the transition state followed by dioxolene ring closure on the downhill part.

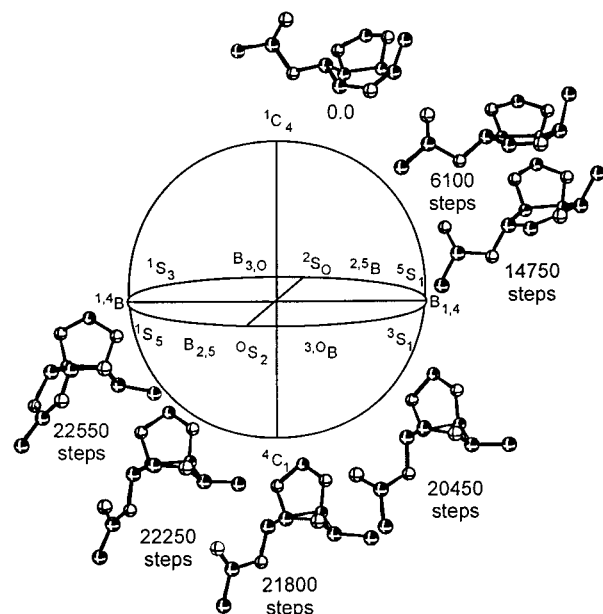


Figure 3. Snapshots of the trajectory connecting **1** and **2**.

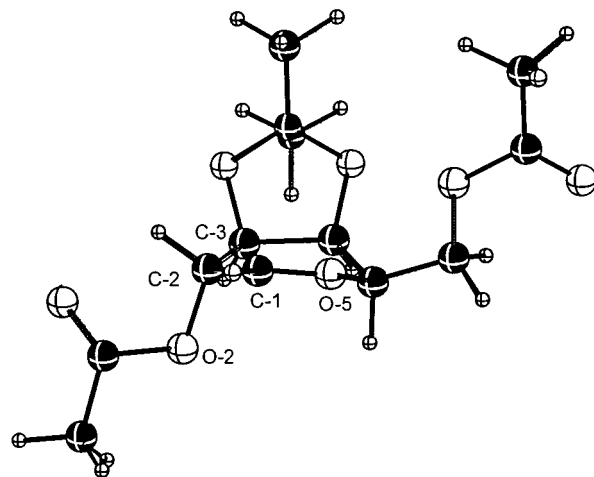


Figure 4. Representation of the transition state connecting **1** and **2**.

Constrained ab initio molecular dynamics methods can help to qualitatively characterize such complicated reactions, but free energies would not be reliable with our method since two different normal modes dominate the first and last part of the trajectory. Stationary points can be determined by optimizing the geometry of candidate structures taken from the dynamical trajectory. The highest energy TS on the minimum energy path is shown in Figure 4 and characterized as the 0S_2 conformation, 34 kJ mol^{-1} above the energy of **1**. Alternative reaction pathways starting with opposite pseudorotation or with the 2-*O*-acyl group rotation lead to high-energy states and not toward **2**.

Our result is somewhat biased by the 3,4-*O*-isopropylidene group but some of the factors responsible for the significant barrier are more general: (1) For hexoses with O-2 equatorial the related oxocarbenium ions adopt an initial conformation with the 2-*O*-acyl group in the equatorial position and oriented syn to H-2. (2) The formation of the neighboring group assisted ion requires a conformational change that moves the 2-*O*-acyl group from an equatorial into an axial position. (3) Visual examination of the dynamics trajectory suggests that the equatorial-axial change is restricted by repulsion between the 2-*O*-acyl group and the protecting groups on O-3. Thus neighboring group participation involves a significant barrier.

(37) Lemieux, R. U. *Chem. Can.* **1964**, *16*, 14.

Our hypothesis is that the stereochemical control of glycosylation reactions could arise from face discriminated nucleophilic attack on ions such as **1**. This can only be true if this S_N1 -like barrier is of comparable or lower energy than the barrier of the competing reaction, ring closure to **2**. Richard et al. have determined the benchmark barrier for a nucleophilic addition to the acetophenone oxocarbenium ion in water as 27.2 kJ mol⁻¹.³⁸ Considering the electronic and solvation effects in a typical glycosylation reaction, the barrier to direct nucleophilic attack on **1** should be lower and thus in principle it can compete with cyclization to **2**.

We consider these results as a major step toward understanding the role of conformation to the kinetic stability of oxocarbenium ions in glycosylation reactions.³⁹ Factors such as the lifetime of oxocarbenium ions,⁴⁰ ion-pairing,⁴¹ solvent,⁴² covalent intermediates,⁴³ etc. all affect the stereochemical outcome of glycosylation reactions. However, at present we want to stress the importance of the conformation of oxocarbenium ions since the energetics and structures of this effect have received little attention.⁴⁴ These conformational preferences may have effects which extend past chemical glycosylation reactions. For example, the hydrolysis of oligosaccharides as catalyzed by some glycosidases has been shown to proceed through intermediates with considerable oxocarbenium ion character.⁴⁵ In several cases

the conformations of such intermediates have been determined to have boat or twist-boat conformations.⁴⁶ In the absence of the enzyme such conformations can interconvert by pseudorotation. It follows from our results that such enzymes must have selected only one of the conformations available to the oxocarbenium ions to stabilize.⁴⁷ Therefore, the design of cationic TS mimics as glycosidase inhibitors should consider the particular conformations available and the barriers to their interconversions. Current efforts have been directed toward synthesizing mimics with a flattened shape but not at those with specific boat or twist-boat shapes.⁴⁸ Similarly the mechanistic studies of glycosyl transferases also suggest intermediates with considerable oxocarbenium ion character.⁴⁹ The new procedures described in this report should be useful in the design of TS state mimics for this class of enzymes too, since they allow for the determination of the important stationary points.

Acknowledgment. This paper is issued as NRC No. 42436.

Supporting Information Available: Tables of experimental data (PDF). This material is available free of charge via the Internet at <http://pubs.acs.org>.

JA001194L

(38) (a) Richard, J. P.; Williams, K. B.; Amyes, T. L. *J. Am. Chem. Soc.* **1999**, *121*, 8403. (b) Richard, J. P. *Tetrahedron* **1995**, *51*, 1535.

(39) (a) Crich, D.; Sun, S. *Tetrahedron* **1998**, *54*, 8321. (b) Crich, D.; Cai, W.; Dai, Z. *J. Org. Chem.* **2000**, *65*, 1291. (c) Lergenmüller, M.; Nukada, T.; Kuramochi, K.; Dan, A.; Ogawa, T.; Ito, Y. *Eur. J. Org. Chem.* **1999**, 1367. (d) Weingart, R.; Schmidt, R. R. *Tetrahedron Lett.* **2000**, *41*, 8753.

(40) (a) Amyes, T. L.; Jencks, W. P. *J. Am. Chem. Soc.* **1989**, *111*, 7888. (b) Zhu, J.; Bennet, A. J. *J. Am. Chem. Soc.* **1998**, *120*, 3887.

(41) Sinnott, M. I.; Jencks, W. P. *J. Am. Chem. Soc.* **1980**, *102*, 2026.

(42) Demchenko, A.; Stauch, T.; Boons, G. J. *SYNLETT* **1997**, 818.

(43) (a) Garcia, B. A.; Gin, D. Y. *J. Am. Chem. Soc.* **2000**, *122*, 4269.

(b) Crich, D.; Sun, S. *J. Am. Chem. Soc.* **1997**, *119*, 11217.

(44) For example: (a) Vermeer, H. J.; van Dijk C. M.; Kamerling, J. P.; Vliegthart, J. F. G. *Eur. J. Org. Chem.* **2001**, 193. (b) Boschi, A.; Chiappe, C.; De Rubertis, A.; Ruasse, M. F. *J. Org. Chem.* **2000**, *65*, 8470.

(45) (a) Heightman, T. D.; Vasella, A. T. *Angew. Chem., Int. Ed. Engl.* **1999**, *38*, 751. (b) Withers, S. G. *Can. J. Chem.* **1999**, *77*, 1.

(46) (a) Williams, S. J.; Hoos, R.; Withers, S. G. *J. Am. Chem. Soc.* **2000**, *122*, 2223. (b) Sulzenbacher, G.; Driguez, H.; Henrissat, B.; Schüle, M.; Davies, G. J. *Biochemistry* **1996**, *35*, 15280. (c) Brameld, K. A.; Goddard, W. A., III *J. Am. Chem. Soc.* **1998**, *120*, 3571.

(47) Hansen, S. U.; Bols, M. *J. Chem. Soc., Perkin Trans 2* **2000**, 665.

(48) (a) Ganem, B.; Papandreou, G. *J. Am. Chem. Soc.* **1991**, *113*, 8984. (b) Lorthiois, E.; Meyyappan, M.; Vasella, A. *J. Chem. Soc., Chem. Commun.* **2000**, 1829.

(49) (a) Ünligil, U. M.; Rini, J. M. *Curr. Opin. Struct. Biol.* **2000**, *10*, 510. (b) Tvaroska, I.; André, I.; Carver, J. P. *J. Am. Chem. Soc.* **2000**, *122*, 8762. (c) Murray, B. W.; Wittmann, V.; Burkart, M. D.; Hung, S. C.; Wong, C. H. *Biochemistry* **1997**, *36*, 823. (d) Müller, B.; Schaub, C.; Schmidt, R. *Angew. Chem., Int. Ed. Engl.* **1998**, *37*, 2893.

(50) Ross, B. D.; True, N. S. *J. Am. Chem. Soc.* **1983**, *105*, 1382.

(51) Pickett H. M.; Strauss, H. L. *J. Am. Chem. Soc.* **1970**, *92*, 7281.